RSC Advances

PAPER

Cite this: *RSC Adv.*, 2020, **10**, 10155

Non-cytotoxic, temperature-responsive and antibacterial POEGMA based nanocomposite coatings with silver nanoparticles†

Svyatoslav Nastyshyn,[a] Joanna Raczkowska,*[a] Yurij Stetsyshyn,*[b] Barbara Orzechowska,[c] Andrzej Bernasik,[d] Yana Shymborska,[b] Monika Brzychczy-Włoch,[e] Tomasz Gosiewski,[e] Ostap Lishchynskyi,[b] Halyna Ohar,[b] Dorota Ochońska,[e] Kamil Awsiuk[a] and Andrzej Budkowski[a]

Received 24th December 2019
Accepted 28th February 2020

DOI: 10.1039/c9ra10874b

rsc.li/rsc-advances

Non-cytotoxic, temperature-responsive and antibacterial poly(di(ethylene glycol)methyl ether methacrylate) – POEGMA188 based nanocomposite coatings attached to a glass surface were successfully prepared using ATRP polymerization. The thickness, morphology and wettability of the resulting coatings were analyzed using ellipsometry, AFM and contact angle measurements, respectively. The strong impact of the thicknesses of the POEGMA188 grafted brush coatings and content of AgNPs on the morphology and temperature-induced wettability changes of the nanocomposite was demonstrated. In addition to the strong temperature-dependent antibacterial activity, the proposed nanocomposite coatings have no significant cytotoxic effect towards normal cells. Moreover, the slight anti-cancer effect of AgNPs may be suggested.

1. Introduction

Silver nanoparticles (AgNPs) are one of the most famous antibacterial agents and demonstrate their properties even against multidrug-resistant bacteria. Due to remarkable optical, electrical and antimicrobial properties, AgNPs have promising applications in biotechnology and life sciences.[1–3] Over the last years the development of modern technologies, which allow for the production of AgNPs of different sizes and shapes, is of great importance[4–6] as it provides an easy way to modify their properties. In addition, the interactions between mammalian cells and Ag-NPs[7,8] are of crucial importance, and strong dependence of the cytotoxicity and geno-toxicity on Ag-NPs functionalities and the type of cells have been demonstrated in recent studies.[7,8]

Composite materials including AgNPs were fabricated using matrix polymers, thin polymer films, gels and microgels, capsules and grafted coatings.[9–21] Remarkable work by R. Fakhrullin's group reported silver nanoparticle-coated "cyborg" microorganisms, which can be used not only to deliver nanoparticles into organisms, but also for the fabrication of smart antibacterial coatings.[22] In turn, the remote activation of capsules containing Ag nanoparticles and infrared dye by laser light was described by Skirtach and co-workers.[23] Special interest is paid to smart antibacterial surfaces because they prevent bacterial attachment and biofilm formation especially using a promising "kill-release" strategy. In this approach, smart materials are able to kill bacteria attached to their surface and then undergo an on-demand release of the dead bacteria and other biological components to reveal a clean surface under an appropriate stimulus, thereby maintaining effective long-term antibacterial activity.[24–26] Silver-polymer nanocomposites with antimicrobial and non-fouling properties were presented by Hu and coworkers[27] and Yang and co-workers.[28] In turn, Ag-nanoparticle-loaded hydrogel coatings with thermoresponsive antibacterial properties were described by He and co-workers,[24] where AgNPs are embedded in cross-linked *N*-isopropylacrylamide and sodium acrylate coating grafted to the substrate.

In our previous works we have described a new method of fabrication of the "command" antibacterial surfaces with temperature-switched killing of the bacteria.[29,30] The coatings were based on silver nanoparticles (AgNPs) embedded in temperature-responsive poly(di(ethylene glycol)methyl ether

[a]*Smoluchowski Institute of Physics, Jagiellonian University, Łojasiewicza 11, 30-348 Kraków, Poland. E-mail: joanna.raczkowska@uj.edu.pl*

[b]*Lviv Polytechnic National University, St. George's Square 2, 79013 Lviv, Ukraine. E-mail: yrstecushun@ukr.net*

[c]*Institute of Nuclear Physics Polish Academy of Sciences, Radzikowskiego 152, 31-342 Kraków, Poland*

[d]*Faculty of Physics and Applied Computer Science, Academic Centre for Materials and Nanotechnology, AGH University of Science and Technology, Al. Mickiewicza 30, 30-049 Kraków, Poland*

[e]*Chair of Microbiology, Department of Molecular Medical Microbiology, Faculty of Medicine, Jagiellonian University Medical College, Czysta 18, 31-121 Kraków, Poland*

† Electronic supplementary information (ESI) available. See DOI: 10.1039/c9ra10874b

methacrylate) – (POEGMA188) as well as in poly(4-vinylpyridine) – (P4VP) coatings attached to a glass surface. Detailed analysis of their properties, performed using numerous surface-sensitive techniques, showed strong impact of the chemical nature of the grafted polymer brushes on the shape of the silver nanoparticles. Moreover, the very effective temperature-switched killing of the bacteria was demonstrated for *Escherichia coli* and *Staphylococcus aureus*.

Motivated by the strong progress within research in the field of smart antibacterial polymeric materials,[23–28] we decided to conduct systematic studies aimed at finding the main regularities between the experimental conditions of the fabrication of the POEGMA188 based nanocomposite coatings with AgNPs and their properties. For this purpose, the AgNPs embedded in POEGMA188 coatings with different thicknesses attached to a glass surface were prepared using ATRP polymerization. AgNPs were synthesized using Ag ions adsorbed into the polymer coatings and reduced to AgNPs by sodium borohydride. Morphology and wettability of the resulting coatings were studied in details using atomic force microscopy (AFM) and measurements of wetting contact angles (CA), respectively. One of the main issues studied in this work was an influence of the fabrication condition of the nanocomposite coatings with AgNPs on their temperature-responsive properties. Obtained results imply that above some threshold values of the silver abundance temperature-responsive properties of the POEGMA188 coatings are no longer preserved. X-ray photoelectron spectroscopy (XPS) analysis implies prolonged release of silver ions from the POEGMA188 coatings caused by the bonding of the AgNPs to the polymer brushes and limiting therefore their possibility to relocate to the human body and making them very prospective materials for human-related applications.

Temperature-depended antibacteriality was demonstrated here for model bacterial strains (*S. aureus* and *E. coli*), confirming our previous results.[30] Additionally, the impact of nanocomposite coatings on mammalian cells was examined. For this purpose proliferation of healthy and cancerous cells was analyzed for two cell lines. They were *in vitro* spontaneously transformed keratinocytes from histologically normal skin (HaCaT) and WM35 cell line derived from the primary melanoma site of the patient's skin diagnosed with radial growth phase (RGP) melanoma. The results indicate that the impact of AgNPs is highly cell-dependent. The anti-cancer impact of AgNPs, postulated by the literature data, reporting their higher cytotoxicity against cancer cells over normal cells[31,32] cannot be proven by the obtained data. However, our research shows that AgNPs embedded in polymer brushes do not have any cytotoxic effect towards normal cells for short exposure times and start to affect them for longer times. This effect might be related with potential long-term release of AgNPs from the grafted brushes and their subsequent accumulation in cells.[7,8,31,33,34]

2. Experimental section

2.1. Materials

2-Bromoisobutyryl bromide – (ATRP initiator), (3-aminopropyl) triethoxysilane – (APTES), (di(ethylene glycol)methyl ether methacrylate) – (OEGMA188), $CuBr_2$, 2,2′-dipyridyl (bpy), triethylamine (Et_3N), sodium L-ascorbate, silver nitrate ($AgNO_3$), sodium borohydride ($NaBH_4$) and solvents were supplied by Sigma-Aldrich.

2.2. Fabrication of nanocomposite coatings

2.2.1 Modification of glass surfaces with ATRP initiator.[35] Glass plates (20 × 20 mm) were placed in a vacuum desiccator or vacuum oven with a vial containing 10 drops of APTES. The chamber was then pumped down to <1 mbar, isolated from the pump and left under a vacuum for 30 minutes. Substrates were then annealed at 110 °C in air at atmospheric pressure for 30 minutes.

After annealing, substrates can be reacted directly with 2-bromoisobutyryl bromide. For this, 10 mL anhydrous tetrahydrofuran was mixed with 2-bromoisobutyryl bromide (0.26 mL, 2.10 mmol) and anhydrous triethylamine (0.30 mL, 2.10 mmol) and were then added to a amino functionalized substrate.

2.2.2 Polymerization of POEGMA188 brushes (surface initiated activators regenerated by electron transfer atom transfer radical polymerization (SI-ARGET ATRP)).[35] The procedure of modification is sketched in Scheme 1. Glass plates with grafted ATRP were placed in test tubes, deoxygenated by nitrogen purging or vacuum/nitrogen cycling. In a round-bottomed flask sealed with a septum, methanol (16 mL), water (4 mL) and di(ethylene glycol)methyl ether methacrylate (34.8 g, 186.0 mmol) were mixed and deoxygenated by bubbling through nitrogen for 10–15 minutes. $CuBr_2$ (7.4 mg, 0.033 mmol), 2,2′-dipyridyl (51.5 mg, 0.33 mmol) and sodium L-ascorbate (65.3 mg, 0.33 mmol) were added and the headspace was purged with nitrogen. The mixture was stirred to dissolve

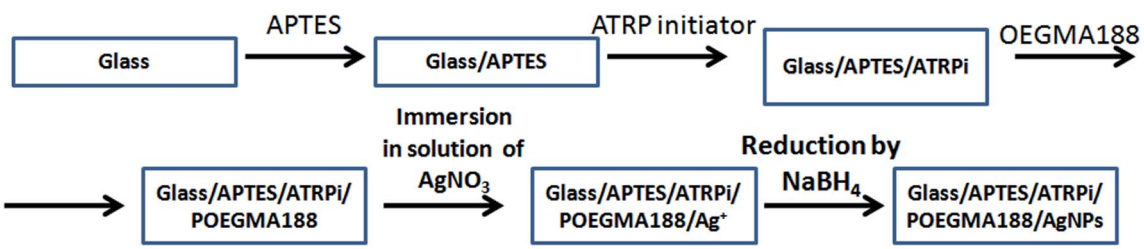

Scheme 1 Fabrication of the nanocomposite coatings based on AgNPs embedded in temperature-responsive POEGMA188 grafted polymer brush.

the solids. Subsequently, the solution was syringed over the substrates in the deoxygenated tubes, or simply poured over the substrates in a screw-top jar, which was then resealed. The samples were allowed to polymerize at ambient temperature. After the different time of the polymerization (2, 5, 16, 26 and 48 h), the samples were removed and washed with ethanol and water.

2.2.3 Incorporation of Ag-NPs onto grafted polymer brushes. Glass plates with grafted polymer brushes were dipped in aqueous $AgNO_3$ solution with different concentrations (5 or 3 mM) for different times (10, 15, 30 and 60 min) under argon flow. Thereafter, the substrates were removed and quickly dipped into an aqueous 0.2 M $NaBH_4$ solution for 12 h. Finally, the substrates were washed several times with distilled water, dried under argon, and used for characterizations.

2.3. Characterization of nanocomposite coatings

2.3.1 X-ray photoelectron spectroscopy analysis (XPS). The X-ray photoelectron spectroscopy measurements were performed with a PHI VersaProbe II apparatus. The samples were irradiated with a focused monochromatic Al Kα ($E = 1486.6$ eV) X-ray beam with a diameter of 100 μm, and the beam was rastered over the area of 400 × 400 μm^2. Analyzer's pass energy was set to 46.95 eV and double neutralization with electrons and low energy monoatomic Ar^+ ions was used to avoid charging effects. Data analysis software from PHI MultiPak was used to calculate elemental compositions from the peak areas.

2.3.2 Water contact angle measurements (CA). Static contact angle measurements were performed by means of the sessile drop technique using a KrussEasyDrop (DSA15) instrument. To determine the thermal response of the grafted brush coatings, the Peltier temperature-controlled chamber was used to carry out the measurements at temperatures ranging from 8 to 35 °C. The temperature was measured by a thermocouple in contact with the sample surface. Contact angle values were collected from 10 different spots and expressed as the average.

2.3.3 Atomic force microscopy (AFM). The commercially available Agilent 5500 system (Keysight) was used to examine the surface topography. The measurements were performed in air, using the non-contact mode with non-coated super sharp silicon probes.

2.3.4 Ellipsometry. The thickness of polymer brushes was measured using the spectroscopic ellipsometer (SENTECH SpectraRey/3) equipped with a micro spot. The ellipsometric angles Ψ and Δ were determined for wavelengths λ in a spectral range between 320 and 800 nm. The measurements were taken at angles of incidence and detection of 56° and 70°. The polymer layers were modeled as a Cauchy layer of thickness d with an refractive index $n(\lambda)$ of the form:

$$n(\lambda) = n_0 + n_1\lambda^{-2} + n_2\lambda^{-4}$$

Layer thickness d and the set of n_0, n_1, n_2 parameters were varied numerically in order to achieve the best agreement between the model and the measured values $\Delta(\lambda)$ and $\Psi(\lambda)$. Refractive indices of the glass substrates were measured independently within the same spectral range and were accounted for in the model.

The typical thickness of the grafted APTES, measured by ellipsometry for the conditions used for glass functionalization, was equal to 0.5 nm.[36,37] The thickness of ATRP films did not exceed 1 nm.

2.4. Antibacterial test

2.4.1 Two reference bacterial strains were used in this study. *Escherichia coli* ATCC 25922 (representative of Gram-negative bacteria) and *Staphylococcus aureus* ATCC 25923 (representative of Gram-positive bacteria). McFarland standard no. 0.5 was used as a reference to adjust the turbidity of two bacterial strains (separately) suspension cells to approximately 5×10^6 CFU mL^{-1} (colony forming unit). In suspensions of both strains, at a volume of 16 mL in Falcon 50 tubes (Axygen), the samples were incubated for 24 hours at 4 °C and 37 °C. Afterward, using a serial dilution method, the bacterial cells were inoculated on Mueller–Hinton agar (Oxoid) and cultured for 24 h at 37 °C.

2.5. Cell culture

Two cell lines were used in this study, keratinocytes from histologically normal skin (HaCaT) and WM35 cell line from the primary melanoma site of the patient's skin diagnosed with radial growth phase (RGP) melanoma. HaCaT cells were cultured in the EMEM (Eagle's Minimum Essential Medium, LGC Standards) and WM35 cells were cultured in the RPMI-1640 (cell culture medium developed at Roswell Park Memorial Institute in 1966 by Moore and his co-workers), both supplemented with a 10% heat-inactivated fetal bovine serum (FBS, Sigma-Aldrich) and 1% antibiotics (Penicillin–Streptomycin–Neomycin Solution Stabilized, Sigma) in culture flasks, in a CO_2 incubator providing 95% air/5% CO_2 atmosphere. The POEGMA188 grafted brush coatings with and without AgNPs embedded were put into the Petri dish (35 mm in diameter) and sterilized for 3 minutes in 99.8% ethanol (POCH, Gliwice). After sterilization, a solution with cells (80 000 cells per mL in the culture medium) was placed over the coatings. Next, the Petri dish was moved into the CO_2 incubator for 1, 3 and 6 days. The experiments were repeated at least twice for each cell line and a time-point.

3. Results and discussion

In the presented work the "smart" nanocomposite brush coating based on AgNPs embedded in temperature-responsive POEGMA188 grafted polymer brush were fabricated (Scheme 1). First, grafted temperature-responsive polymer brushes with different thicknesses were fabricated in a three-step process, for the glass surface previously functionalized by APTES and then ATRP molecules. The thicknesses of grafted coatings were tuned by the time of the ATR polymerization of POEGMA188. Subsequently, Ag ions were adsorbed into the polymer coating and reduced to AgNPs by sodium borohydride.[29,30] It is important to note, that the "freshness" of the sodium borohydride is

of a crucial impact on the amount of the synthesized AgNPs. Therefore, only freshly opened reagent was used here.

The thickness, morphology and wettability of the resulting coatings were analyzed using ellipsometry, AFM and CA measurements, respectively. In addition, the impact of the thickness of the POEGMA188 grafted brush coatings and content of AgNPs on the morphology and temperature-induced wettability were examined and described in details in Section 3.1. In turn, the antibacterial properties and cytotoxic influence of the POEGMA188 coatings with embedded AgNPs on healthy keratinocytes (HaCaT) and cancerous WM35 cell lines are presented in Section 3.2.

3.1. Fabrication and characterization of the POEGMA188 based nanocomposite brush coatings with AgNPs: morphology and temperature-responsive properties

POEGMA188 based nanocomposite brush coatings with silver AgNPs were fabricated using different experimental conditions, listed in Table 1. Resulting POEGMA188 coatings with different thickness, tuned by adjustment of polymerization time (Table 1), were used as templates for synthesis of the AgNPs. In addition, glass decorated with APTES was used as a reference. By changing the time of the immersion of the POEGMA188 coatings in $AgNO_3$ solution as well as the concentration of the $AgNO_3$ we were able to modify significantly the properties of the nanocomposite brush coatings.

Thickness and refractive index of grafted coatings were examined using ellipsometry. Typical thickness of APTES, measured by ellipsometry was equal to 0.5–1.5 nm (in accord with literature[36,37]). In turn, the thickness of the ATRP coating used as a substrate for POEGMA188 polymerization was equal to approximately 1 nm. The average thickness of the POEGMA188 grafted brush coatings in a dry state at room temperature (20 °C) depends strongly on polymerization time and is in the range from 0 to 86 nm (Fig. S1†). In turn, refractive index of the "pure" POEGMA188 coatings is in the range of 1.50–1.54. The incorporation of AgNPs into the POEGMA188 polymer matrix has very weak impact on the thickness of POEGMA188 coatings, in contrary to the refractive indexes which increases significantly and approach the values varying from 1.59 to 1.63.

Table 1 Experimental conditions for fabrication of the POEGMA188 based nanocomposite brush coatings with silver AgNPs

Samples of the POEGMA188 brush coatings with different polymerization times	Concentration of the $AgNO_3$ in solution and time of the immersion			
	3 mM	5 mM		
	15 min	15 min	30 min	60 min
APTES		+		
POEGMA 2 hours		+		
POEGMA 5 hours		+	+	+
POEGMA 16 hours	+	+	+	+
POEGMA 26 hours		+		

POEGMA188 brushes are able to change their properties sharply upon relatively small temperature changes due to the coil–globule transition in aqueous solutions at the low critical solution temperature. To investigate temperature-induced switching of wetting properties and the impact of the AgNPs on this process, the contact angles of sessile water droplets on the grafted brush coatings were measured between 5 and 34 °C for POEGMA188 (Fig. 1a). Except for very thin POEGMA layers, corresponding to the weak modification (polymerization time – 2 hours and thickness nearly 10 nm, blue symbols), all other POEGMA188 coatings exhibit well expressed transitions of wetting properties described by Boltzmann's curves, observed for temperatures between 16–19 °C. In contrast, no sharp transition in contact angles recorded for surface functionalized by APTES and ATRP initiator (Fig. 1a, green open diamantes) was observed. Fig. 1b shows temperature dependences of water contact angles determined for "pure" POEGMA188 coatings fabricated for the polymerization time equal to 5 hours (thickness nearly 30 nm, red open squares) as well as with AgNPs embedded into polymer matrix after 15 min (violet solid squares) and 30 min (blue solid circles) of the silver immobilization at 5 mM $AgNO_3$ concentration in solution and followed by reduction in 0.2 M $NaBH_4$ solution for 12 h. Recorded results show, that nanocomposite coatings with embedded AgNPs, especially the ones prepared after 30 min immobilization in $AgNO_3$ solution, are more hydrophilic than the "pure" POEGMA188 coating. For both coatings with embedded AgNPs only a slight increase in hydrophobicity with rising temperature was described as a linear relation. Analogical studies were

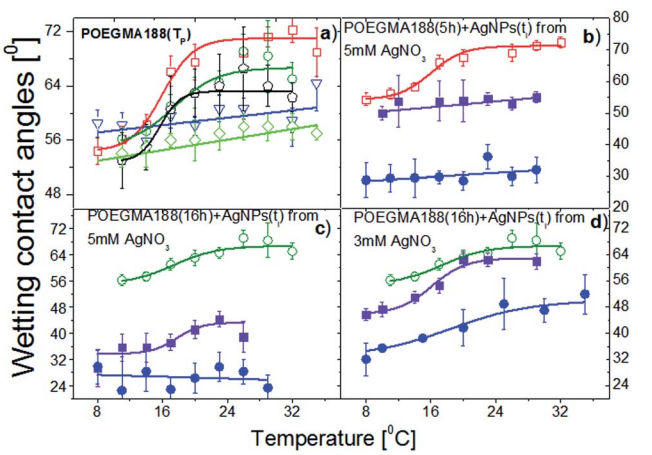

Fig. 1 Temperature dependences of water contact angles determined for the grafted brush coatings POEGMA188 fabricated with different polymerization times T_P, without (a) and with (b–d) AgNPs embedded in the brushes after exposure to 5 mM (b and c) and 3 mM $AgNO_3$ solutions (d) for different immersion times t_i, followed by reduction in 0.2 M $NaBH_4$ solution for 12 h. Conditions of AgNPs synthesis (b–d) are optimized for the POEGMA188 coatings obtained after 5 h (b) and 16 h (c and d) of polymerization. The data corresponding to different polymerization times ($T_P = 0$ h), green open diamantes; 2 h, blue open triangles; 5 h, red open squares; 16 h, olive open circles; 26 h, black open pentagons and non-zero AgNP synthesis times ($t_i = 15$ min, violet solid squares; 30 min, blue solid circles) are marked by open and solid symbols, respectively.

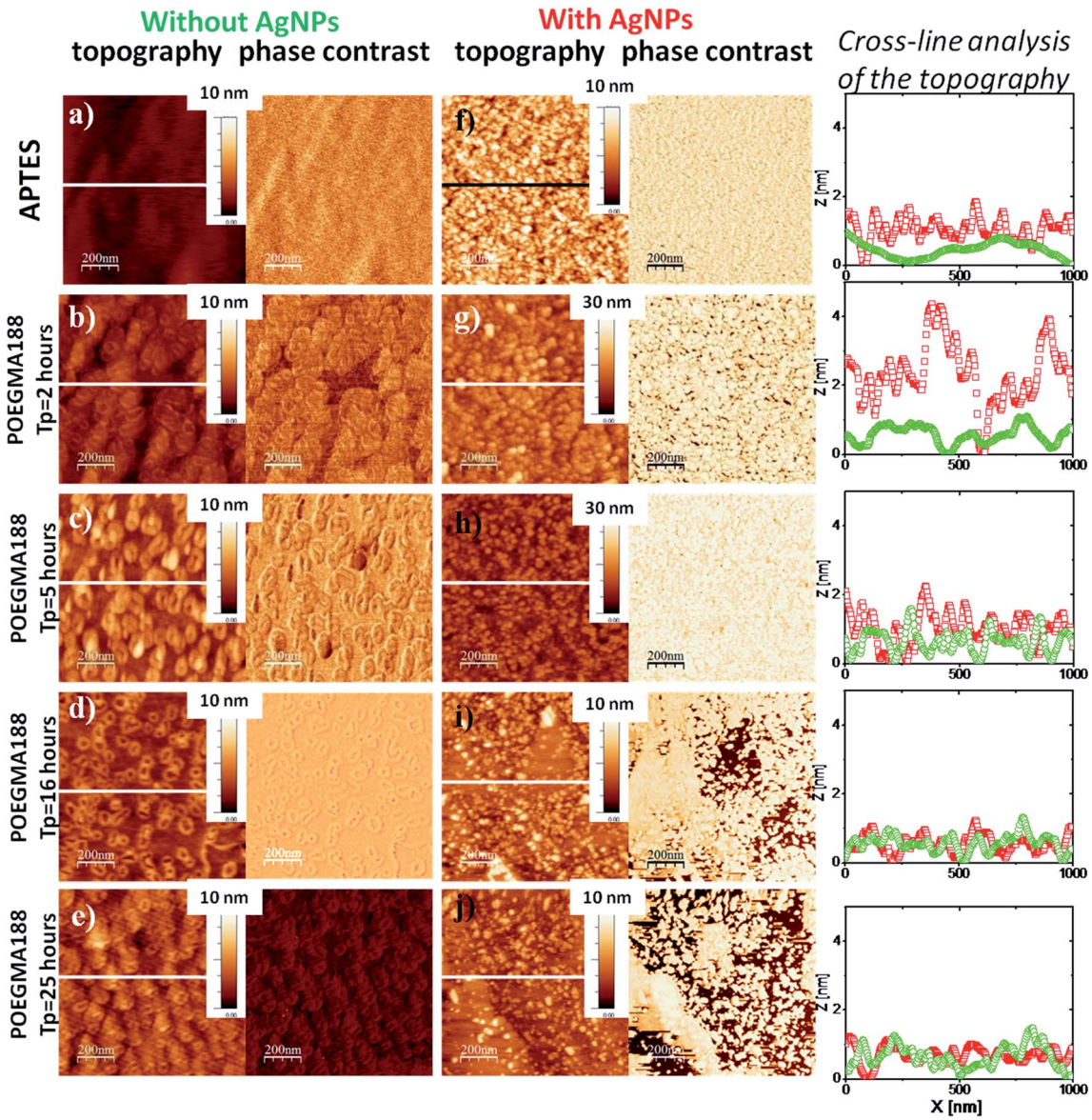

Fig. 2 Representative AFM images (topography and phase contrast, recorded in a dry state) of the glass surface silanized with APTES (a) and subsequently functionalized with grafted POEGMA188 brushes (b–e, using different polymerization times T_P), compared with the data for the same substrates incorporating AgNPs (f–j) after a 15 min long exposure to 5 mM $AgNO_3$ solution, followed by reduction in 0.2 M $NaBH_4$ solution for 12 h. Cross-line analysis corresponds to the topography of the samples without (green) and with AgNPs (red).

performed for POEGMA188 coatings fabricated with polymerization time equal to 16 hours (thickness nearly 60 nm), where for nanocomposite coatings with AgNPs synthesized after 15 min of the silver immobilization (Fig. 1c, olive open circles) a sharp transition of wetting properties at 18 °C was recorded. In contrary, for POEGMA188 coatings with AgNPs fabricated for silver immobilization time equal to 30 min, no transition was observed (Fig. 1c, blue solid circles). Although the curves of the temperature dependences of water contact angles determined for the POEGMA188 grafted brush coatings with embedded AgNPs fabricated after 15 min of the silver immobilization as well as the "pure" ones have a similar character, POEGMA188 grafted brush coatings with embedded AgNPs are significantly more hydrophilic than "pure" POEGMA188 coatings. A similar

Table 2 RMS of the grafted polymer brushes coatings in dry state

	RMS [nm]			
		With AgNPs		
		Time of the immersion		
Samples	Without AgNPs	15 min	30 min	60 min
APTES	0.3 ± 0.1	1.8 ± 0.2		
POEGMA 2 hours	0.7 ± 0.1	3.4 ± 0.1		
POEGMA 5 hours	1.3 ± 0.2	2.6 ± 0.2	2.2 ± 0.2	1.5 ± 0.2
POEGMA 16 hours	1.1 ± 0.2	1.5 ± 0.2	0.4 ± 0.2	0.4 ± 0.2
POEGMA 26 hours	1.1 ± 0.1	1.4 ± 0.1		

effect was described by Kasraei and co-workers[38] where the incorporation of silver nanoparticles into composite resins was studied. Metallic nanoparticles have a large surface energy. The nano-sized silver particles have a higher surface energy than micro-sized ones, resulting in an increase of the surface energy of the grafted polymer brush coatings and consequently decreasing the water contact angle.[38] Moreover, a strong dependence between concentration of the embedded AgNPs and temperature-responsive properties of POEGMA188 grafted brush coatings is demonstrated.

To study the influence of the silver nanoparticles on the morphology of the coatings comprehensive AFM analysis was performed for APTES and POEGMA188 coatings with different grafting polymerization time (or different ellipsometry thickness, 0–86 nm). Morphology of the APTES is smooth, with uniform silane coverage (Fig. 2a). In turn, AFM morphologies recorded for all analyzed types of "pure" POEGMA188 coatings without AgNPs (Fig. 2b–e) depict relatively smooth surfaces with small patch structures. Root mean square (RMS) values calculated for the POEGMA188 coatings (Table 2) grow almost four times with polymerization time up to 5 hours (thickness ~ 30 nm) and remain almost constant for longer fabrication times. Moreover, analyzed surfaces do not show any phase contrast.

In contrast, for the samples with incorporated AgNPs (with 15 min immersion in $AgNO_3$ solution) (Fig. 2f–j) well developed, patch structures are clearly visible and the RMS values, increase considerably except the POEGMA188 nanocomposite coatings with polymerization times of 16 and 25 hours where only relatively slight increase in RMS values are shown (see Table 2). RMS value calculated for the APTES coating with embedded AgNPs increased six times, whereas for POEGMA188 coatings after 2, 5, 16 and 26 hours of the polymerization an increase by 4.8, 2, 1.4 and 1.3 times, respectively was observed. The cross-line analysis of the topography for APTES and POEGMA188 coatings with 2 and 5 hours of the polymerization time demonstrates significantly better developed surface for coating

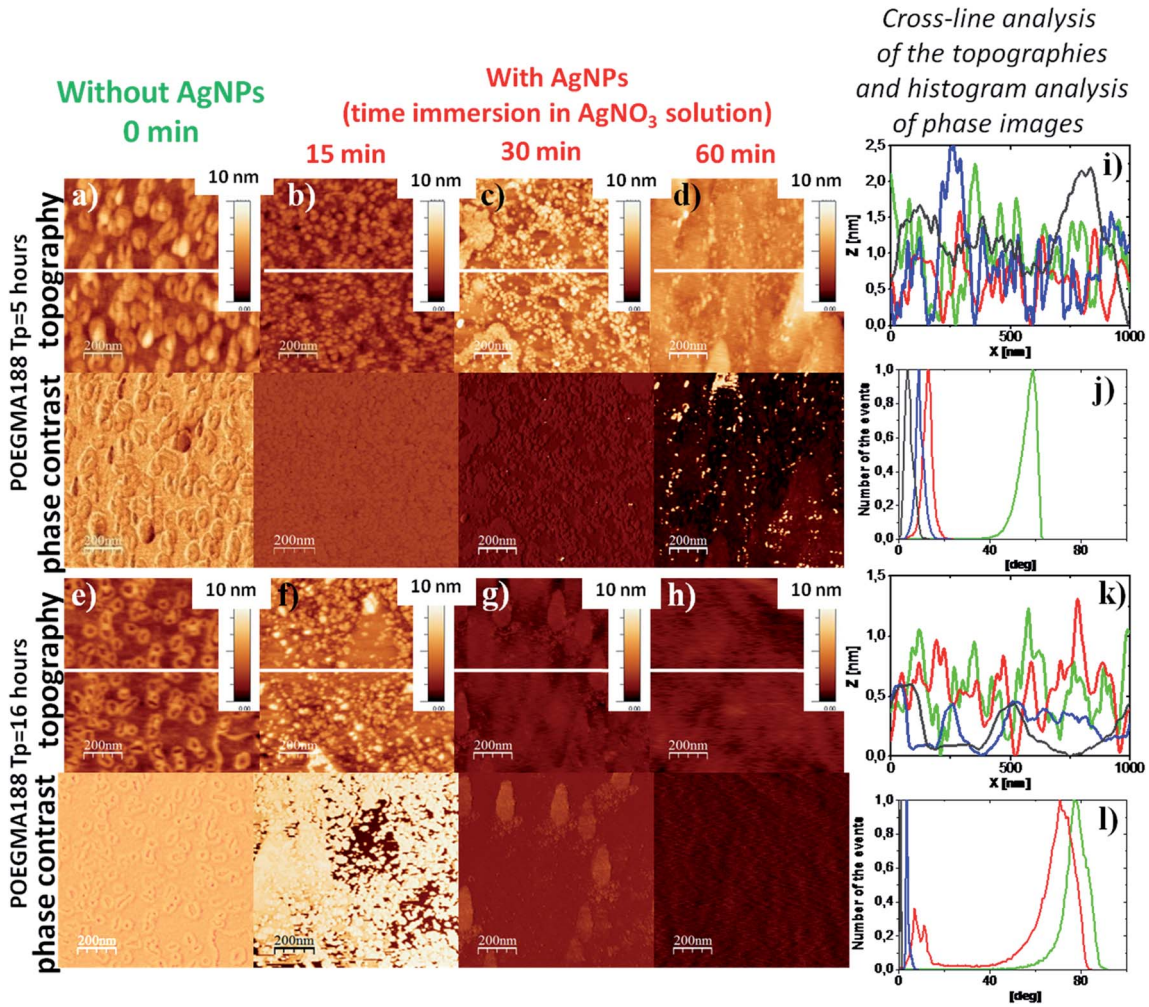

Fig. 3 Typical AFM images (topography and phase contrast, recorded in a dry state) of the grafted brush coatings POEGMA188 fabricated with different polymerization times ($T_P = 5$ h, a–d; $T_P = 16$ h, e–h) prior to (a and e) and after incorporation of AgNPs (b–d and f–h) – resulting from immersion for different times in 5 mM $AgNO_3$ solution, followed by reduction in 0.2 M $NaBH_4$ solution for 12 h. Cross-line analysis of the topographies (i and k) and histogram analysis of phase images (j and l) recorded for the coatings POEGMA188 fabricated with different polymerization time ($T_P = 5$ h, i and j; $T_P = 16$ h, k and l) without (green) and with incorporated AgNPs after 15 min (red), 30 min (blue) and 60 min (black) long silver immobilization.

with AgNPs (red line) suggesting that nanoparticles are at least partially located at the top of the polymer matrix. In contrast, the cross-line analysis of the topography of POEGMA188 coatings with polymerization time of 16 and 26 hours demonstrates higher degree of the topographical homogeneity. However, the phase contrast inhomogeneity visible in this case implies the existence of nanocomposite material where AgNPs are incorporated in the polymer matrix.

Another important factor enabling modification of nanocomposite properties is the time of brush coating immersion in $AgNO_3$ solution. POEGMA188 coatings fabricated after 5 and 16 hours of the polymerization (with thicknesses 31 and 59 nm, respectively) were used to study in detail an impact of the time of immersion in $AgNO_3$ solution (ranging from 0 to 60 min).

The RMS values determined for the POEGMA188 coatings fabricated using 5 hours of polymerization with incorporated AgNPs after 15 min of immersion in $AgNO_3$ solution (Fig. 3b) is doubled as compared to the native coatings (Fig. 3a) (Table 2). In turn, an increase in immersion time from 15 to 30 and 60 min is followed by slight decrease of RMS values. The cross-line analysis of the topographies of these coatings shows similar surface structuring (Fig. 3i). In contrast, histogram analysis of phase images shows essential difference between the POEGMA188 coatings (Fig. 3j, green line) and POEGMA188 brushes with AgNPs incorporated after different times of the immersion in $AgNO_3$ solution (Fig. 3j, red, blue and black lines). This suggests only one phase for nanocomposites with AgNPs and strong metallization of the coatings. Phase imaging allows recognizing regions with different elasticity[39–41] or other structural heterogeneities[41] by recording offsets and phase angles of input signal variations with respect to those of the oscillating cantilever.

For the POEGMA188 coatings with polymerization time equal to 16 hours (Fig. 3e) and AgNPs synthesized after 15 min immersion (Fig. 3f), only slightly increased RMS value is recorded, as compared with the "native" POEGMA188 coatings (Table 2). In contrast, for nanocomposites obtained after 30 and 60 min of immersion in $AgNO_3$ solution (Fig. 3g and h) the RMS values are sharply reduced by almost four times (Table 2). The topographies of these two samples are more homogeneous, which is confirmed also by the cross-line analysis of the topography (Fig. 3k, blue and black lines). Histogram analysis of the phase images demonstrates the properties of the nanocomposite surfaces changing with the amount of silver immobilized from $AgNO_3$ solution (Fig. 3l). "Bare" POEGMA188 coating exhibits one peak on the phase histogram centered around 80 degree (Fig. 3l, green line). The same coating incorporating AgNPs synthesized after 15 min immersion in $AgNO_3$ solution reveals two well expressed peaks (Fig. 3l, red line), one centered around the phase value characteristic for 'bare' POEGMA188 brush (Fig. 3l, green line) and the second peak located close to those characteristic for the nanocomposites with higher amount with immobilized silver (Fig. 3l, blue and black lines, for 30 min and 60 min immersion in $AgNO_3$ solution, respectively). The number of histogram peaks corresponds to the number of separated phases on the surface of the coating, suggesting the two-phase system for the POEGMA188 with AgNPs synthesized after 15 min long immersion in $AgNO_3$ solution, where temperature-responsive properties of the coatings are preserved (Fig. 1c, red line, squares).

3.2. Release of the silver with POEGMA188 based nanocomposite coatings with embedded AgNPs

The applicability of materials containing AgNPs is strongly restricted by their potential cytotoxicity as well as by the tendency to accumulate in human organs. However, this risk should be minimalized for the proposed command surfaces as the AgNPs are bonded to the polymer brushes so their possibility to relocate to the human body should be strongly limited. To verify this issue, we have performed systematic XPS studies

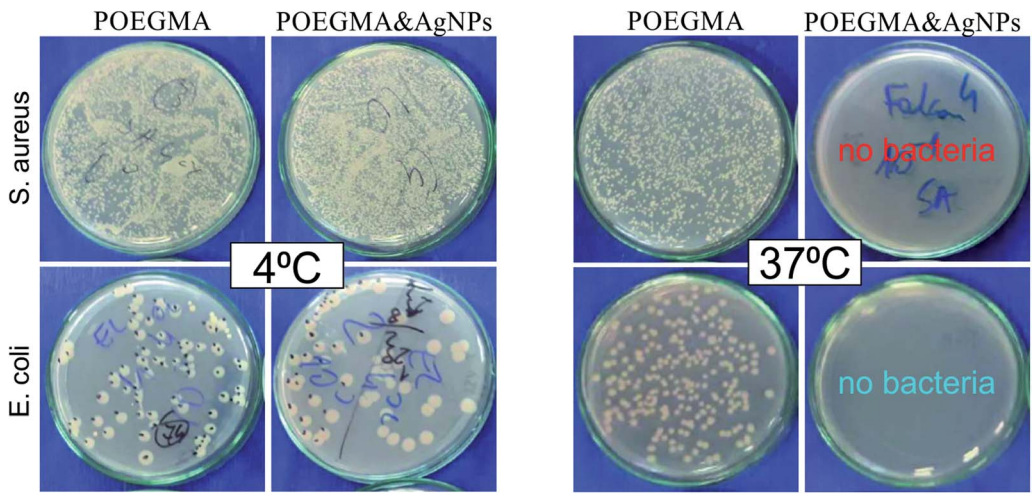

Fig. 4 Antibacterial properties of POEGMA188-based nanocomposite coatings against *E. coli* and *S. aureus*. The Petri plates after incubation for 24 hours at 4 °C (left panel) and 37 °C (right panel) with POEGMA188-based nanocomposite coatings fabricated for 16 hours of polymerization (POEGMA) and with incorporated AgNPs obtained after 15 min of immersion at 5 mM $AgNO_3$ solution followed by reduction in 0.2 M $NaBH_4$ solution for 12 h (POEGMA & AgNPs).

of silver release from produced coatings into the aqueous environment. For this purpose, each sample was measured 'as prepared', and then after immersion in water at room temperature for times ranging up to 55 days. To eliminate the influence of potential statistical variations between the samples, the ratio between the Ag content measured for immersed coating and the initial Ag abundance Ag_0, recorded for 'as prepared' sample was calculated. The results, presented in Fig. S2† show the monotonic decrease of Ag amount in POEGMA-grafted brushes, down to 50% for first 15 days of incubation in water and significant suppression of this effect for longer incubation times. The abundance of Ag does not drop below 35% of initial value even after 55 days of incubation. This effect may be related to a very good isolation of the AgNPs in polymer matrix observed for some critical sizes of AgNPs, not allowing for further release of the silver ions. Moreover, for small sizes of the AgNPs the strong affinity of oxygen from ether groups of the POEGMA188 with silver clusters can be predicted.[42,43]

Observed prolonged release of silver ions from the POEGMA188 coatings suggests that they may be very prospective materials for human-related applications, as they strongly minimalize the risks of negative effects towards human health. However, further studies on Ag release in more physiological conditions, *e.g.* in phosphate saline buffer (PBS) at 37 °C are required.

3.3. Antibacteriality and cytotoxicity of POEGMA188 based nanocomposite coatings with embedded AgNPs

In our previous work[30] we have demonstrated the temperature-switched killing of the bacteria on POEGMA188 and P4VP based

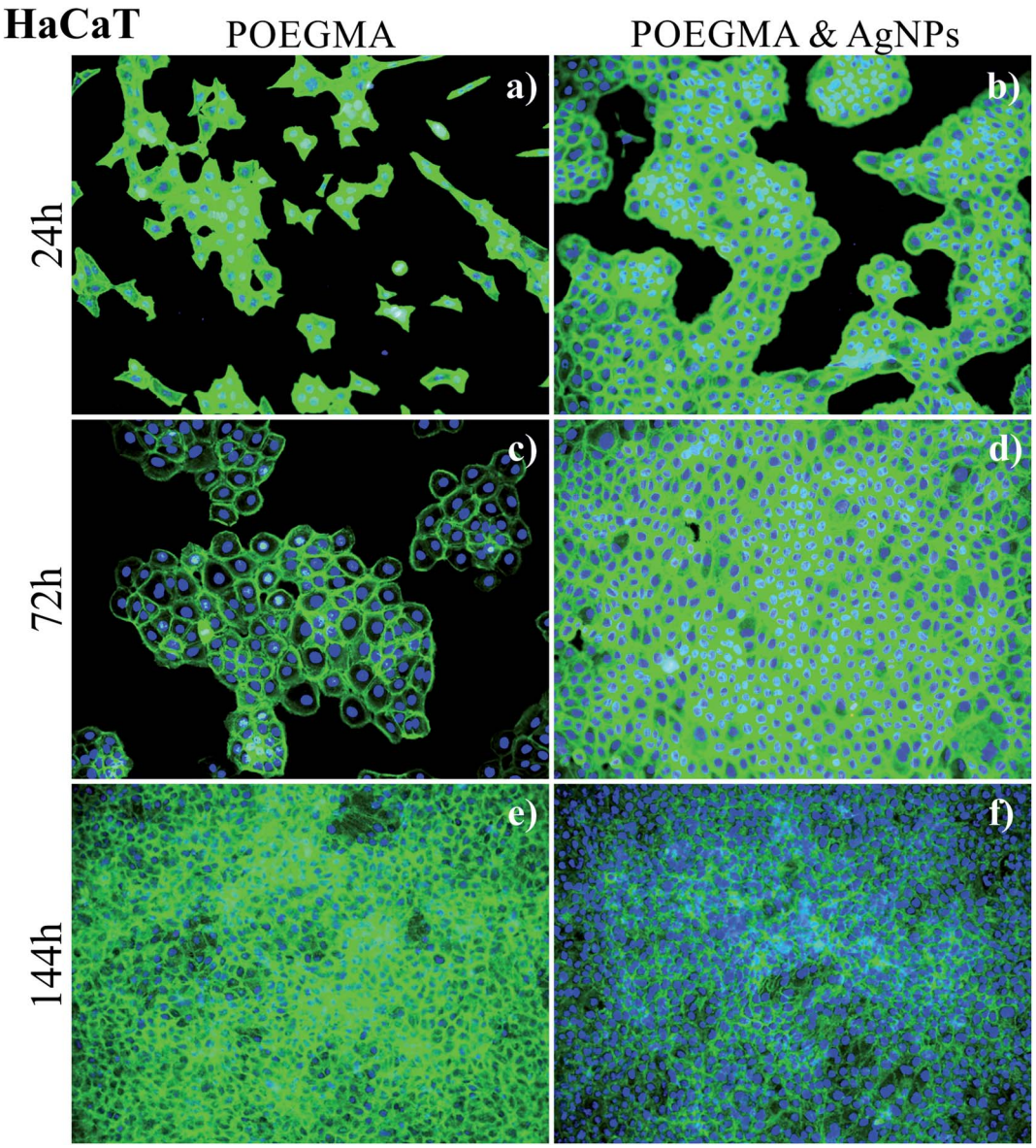

Fig. 5 Growth of healthy HaCaT cells on POEGMA188-based nanocomposite coatings fabricated for 16 hours of polymerization (a, c and e) and POEGMA188 with incorporated AgNPs obtained after 15 min of immersion at 5 mM $AgNO_3$ solution followed by reduction in 0.2 M $NaBH_4$ solution for 12 h (b, d and f).

coatings where no significant difference was observed at 4 °C between the amounts of bacteria counted on the nanocomposite coatings with AgNPs and on the "bare" coating control sample. In contrast, at 37 °C almost no bacteria were visible for temperature-responsive coating with AgNPs, whereas the growth of bacteria remained unperturbed for "pure" coating, indicating well-expressed temperature-dependent antibacterial properties of AgNPs integrated into brushes. Similar results were obtained also for the coatings examined in the present study fabricated with optimized conditions (16 hours of polymerization, 15 min of silver immobilization from 5 mM $AgNO_3$ solution). Fig. 4 demonstrates cultivation of *E. coli* and *S. aureus* model bacterial strains on the Petri plates after incubation with the POEGMA188-based nanocomposites as well as POEGMA188 control samples at 4 °C (left panel) and 37 °C (right panel) that confirms our previous results.[30]

Although AgNPs have astounding pharmacological properties, the possibility of their application is strongly limited by their potential cytotoxicity and genotoxicity, activated by various mechanisms, in particular the production of excess reactive oxygen species (ROS), which results in oxidative stress, reduced levels of glutathione, elevated lipid peroxidation, inflammation, DNA damage, altered cell cycle and proliferation capacity, and apoptosis and necrosis.[33,44–46] AgNPs have also the tendency to accumulate in human organs, like liver, spleen, lungs, and kidney[7,8,31] and they are able to can cross the blood–brain barrier (BBB) and accumulate in different regions of the brain.[34] These effects depend strongly on the shape, size and concentration of AgNPs, as well as on the cell type.[45,47,48]

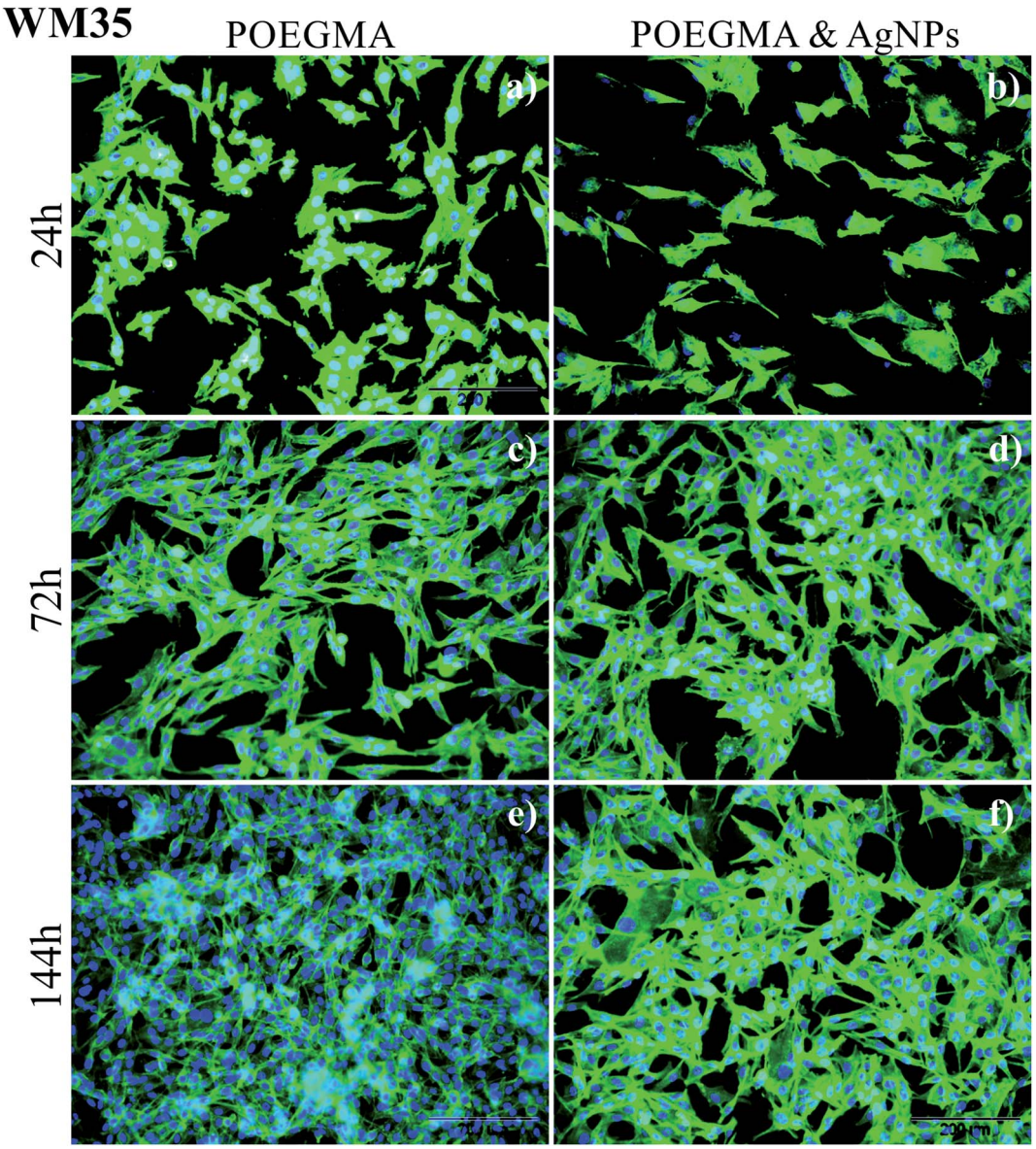

Fig. 6 Growth of cancerous WM35 cells on POEGMA188-based nanocomposite coatings fabricated for 16 hours of polymerization (a, c and e) and POEGMA188 with incorporated AgNPs obtained after 15 min of immersion at 5 mM $AgNO_3$ solution followed by reduction in 0.2 M $NaBH_4$ solution for 12 h (b, d and f).

Although the cytotoxic and differentiation-inducing properties are generally considered as negative, they result in a great anti-cancer impact of AgNPs, since they show higher cytotoxicity against cancer cells in comparison with normal cells.[31,32] Numerous research show, that in cancer chemotherapeutic regimes, AgNPs can promote apoptosis and tumor cell differentiation.[49,50] To minimalize the risks of negative effects towards human health, the materials with prolonged release of silver ions from permanently bonded AgNPs are highly demanded. XPS results (Fig. S2†) indicate that proposed coatings fulfill this requirement. Moreover, according to the literature[51,52] potential hazardous effects of AgNPs depend also on their location in the coating. Based on these criteria, materials may be grouped into three categories: 'expected to cause exposure' for NPs suspended in liquids and airborne NPs, 'may cause exposure' for surface-bound NPs and 'no expected exposure' for NPs suspended in solids.[53] Due to the conformation of polymer brushes, the AgNPs in the studied coatings are dispersed uniformly in the whole brush and not only on the surface, therefore they should fall rather into the third category. What is more, the thermo-responsivity of the coatings limits strongly the possible interactions between AgNPs and the external environment, as they are permitted only at temperatures above LCST.

To study the impact of AgNPs embedded into the POEGMA188 nanocomposite coatings (16 h of polymerization time, 15 min of silver immobilization from 5 mM $AgNO_3$ solution) on proliferation of healthy and cancerous cells, two cell lines were chosen. They were *in vitro* spontaneously transformed keratinocytes from histologically normal skin (HaCaT) and WM35 cell line derived from the primary melanoma site of the patient's skin diagnosed with radial growth phase (RGP) melanoma. Cells were seeded on all substrates using the same initial solution to avoid discrepancies linked with various cellular densities.

Representative fluorescence images recorded after 24, 72 and 144 h culture time, are presented in Fig. 5 for keratinocytes and Fig. 6 for melanoma cells.

The comparison of the growth of healthy (keratinocyte) HaCaT cells on "pure" POEGMA coating (Fig. 5, left panel) and on POEGMA coating with AgNPs (Fig. 5, right panel) suggests that cells grow faster on the polymer brush with nanoparticles, where they form confluent layer already after 72 h of incubation. For the coating without AgNPs, formation of such layer is observed first after 144 h culture time.

In turn, for WM35 cancerous (melanoma) cells (Fig. 6) rather an opposite effect was noticed. The amount of cells is slightly smaller on the POEGMA brushes with AgNPs and after 144 h incubation time they only start to converge. In contrast, on the "pure" polymer coating the monocellular layer is already formed after the same incubation time. These results indicate that AgNPs embedded in polymer brush do not have any significant cytotoxic effect towards normal cells and suggest a slight anti-cancer impact of AgNPs.

To confirm these statements, quantitative analysis was performed, with number of cells as well as proliferation index determined (Fig. 7), the latter defined as the ratio between the number of cells after given incubation time and the number of cells after 24 hours of culture. The number of cells presents on the surface after a given culture time depends on two factors, *i.e.* the number of initially adhered cells and their further ability to proliferate. The proliferation index provides information about the ability of adhered cells to proliferate on the examined surfaces independently of their adhesive properties. For cancerous WM35 cell line, both, the number of cells and proliferation index, are comparable and do not show any noticeable differences independently of the substrate used for the study. In contrast, for healthy keratinocytes (HaCaT), significant, time-dependent impact of AgNPs can be observed. For short incubation times, up to 72 h, the number of HaCaT cells counted for the POEGMA188 coating with embedded AgNPs is approximately 5 times larger for POEGMA coating with embedded AgNPs and at the same time proliferation index is almost doubled in comparison with the "pure" polymer coating.

However, this situation changes for longer incubation time (144 h) such that the number of cells on POEGMA188 coating

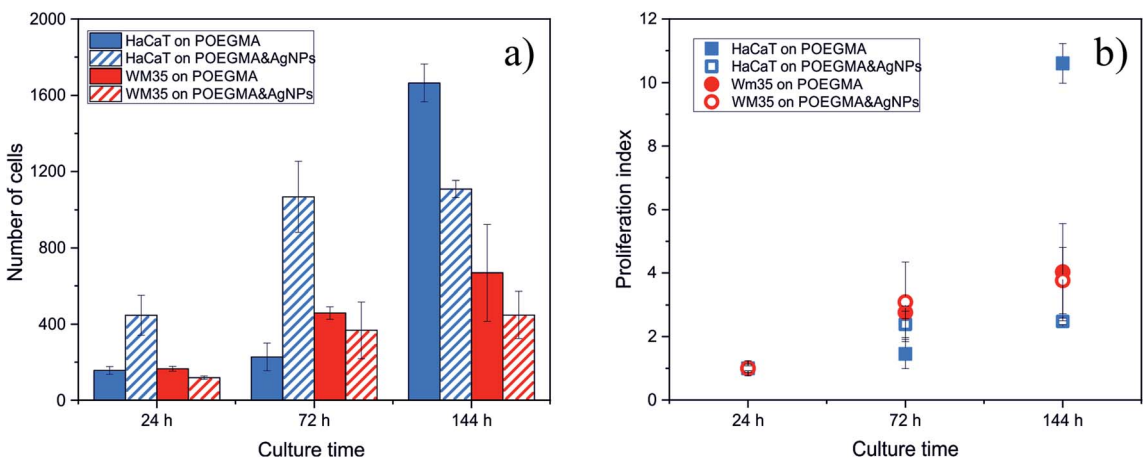

Fig. 7 Impact of AgNPs embedded in POEGMA188 grafted brush coatings on the amount (a) and proliferation index (b) of HaCaT and WM35 cells.

starts to exceed the number of cells on polymer brush with embedded AgNPs, by 25%. This effect is particularly manifested in the value of proliferation index, increasing sharply for cells incubated on POEGMA-grafted brush and remaining almost unchanged for the substrate with AgNPs.

These results indicate that the impact of nanocomposites with AgNPs is highly cell-dependent. The slight decrease of the number of cancerous cells do not allow to confirm an anti-cancer impact of AgNPs, postulated by the literature data, reporting their higher cytotoxicity against cancer cells over normal cells.[31,32] In turn, our research shows that AgNPs embedded in polymer brush do not have any cytotoxic effect towards the normal cells for short exposure times and start to affect them for longer times. This effect might be related with potential long-term release of AgNPs from the grafted brush and their subsequent accumulation in cells.[7,8,31,33,34]

4. Conclusion

In the present work, the non-cytotoxic, temperature-responsive and antibacterial POEGMA188 based nanocomposite coatings attached to a glass surface were successfully prepared using ATRP polymerization. The nanocomposite coatings were fabricated in an easy process, for the glass surface previously functionalized by APTES and subsequently with ATRP molecules. In the next step, POEGMA188 grafted brushes were fabricated and then Ag ions were adsorbed into the coatings and reduced to AgNPs by sodium borohydride.[29,30]

The thickness, morphology and wettability of the resulting coatings were analyzed using ellipsometry, AFM and CA measurements, respectively. The strong impact of the thicknesses of the POEGMA188 grafted brush coatings and the amount of AgNPs on the morphology and temperature-induced wettability of the nanocomposite was demonstrated. Above some threshold concentration of the AgNPs in POEGMA188 coatings, temperature-responsive properties are absent. Based on our previous work[30] and presented here results it can be stated that temperature-responsive POEGMA188 based nanocomposite coatings with silver nanoparticles can be synthesized only for brush thickness larger than 45 nm in a dry state, and for moderate AgNPs concentrations equivalent to Ag^+ immobilization in 5 mM $AgNO_3$ solution no longer than 15 min.

Strong temperature-responsive antibacterial effect of POEGMA188 based nanocomposite was demonstrated here, confirming our previous work.[30] The possibility of application of materials containing AgNPs is strongly restricted, due to their potential cytotoxicity as well as their tendency to accumulate in human organs. However, this risk should be minimalized for the proposed nanocomposite coatings where the AgNPs are bonded to the polymer brushes so their possibility to relocate to the human body should be strongly limited. XPS results have shown prolonged release of silver from the POEGMA188 coatings suggesting release of silver ions and not whole Ag nanoparticles, however abundance of Ag does not drop below 35% of initial value even after 55 days of incubation. Moreover, POEGMA188 nanocomposite coatings have no significant cytotoxic effect towards normal cells examined here and only a slight anti-cancer impact, which confirms our hypothesis that only silver ions are released.

New POEGMA-based nanocomposite grafted brush coatings have at least three advantages. First, the temperature-dependent antibacterial properties have a great potential for applications, from medical laboratories to food packaging, where the intensive growth of microorganisms at elevated temperatures is a natural but undesired process. Second, AgNPs embedded in the polymer brush do not have any cytotoxic effect towards the normal cells for short exposure times. Third, the release of silver ions from the POEGMA188 nanocomposite coatings in water has prolonged character (at least some weeks).

Notes

A patent applications P.424734 (PL, 2018-03-02) and PCT/PL2019/05001 (Patent Cooperation Treaty, 2019-09-06) related to this work have been filed.

Conflicts of interest

All authors have no conflict of interest.

Acknowledgements

This work was partially supported by the Dean of the Faculty of Physics, Astronomy and Applied Computer Science at Jagiellonian University. The authors thank K. Małek-Ziętek from the Centre for Technology Transfer CITTRU at Jagiellonian University for her support during process of legal protection and commercialization of intellectual property. The research was carried out with equipment purchased with financial support from the European Regional Development Fund in the framework of the Polish Innovation Economy Operational Program (Contract no. POIG.02.01.00-12-023/08). Svyatoslav Nastyshyn thanks for financial support from DSC2019 #N17/MNS/000031 and Descartes Project in Jagiellonian University. Yana Shymborska thanks for financial support from Queen Jadwiga Fund.

References

1 J. Kim, E. Kuk, K. Yu, J. Kim, S. Park, H. Lee, S. Kim, Y. Park, Y. Park, C. Hwang, Y. Kim, Y. Lee, D. Jeong and M. Cho, *Nanomedicine*, 2007, **3**, 95.
2 D. Evanoff and G. Chumanov, *ChemPhysChem*, 2005, **6**, 1221.
3 D. Chen, X. Qiao, X. Qiu and J. Chen, *J. Mater. Sci.*, 2009, **44**, 1076.
4 B. Rybak, M. Ornatska, K. Bergman, K. Genson and V. Tsukruk, *Langmuir*, 2006, **22**, 1027.
5 Z. Shervani, Y. Ikushima, M. Sato, H. Kawanami, Y. Hakuta, T. Yokoyama, T. Nagase, H. Kuneida and K. Aramaki, *Colloid Polym. Sci.*, 2008, **286**, 403.
6 M. Moffitt and A. Eisenberg, *Chem. Mater.*, 1995, **7**, 1178.
7 I. Sur, M. Altunbek, M. Kahraman and M. Culha, *Nanotechnology*, 2012, **23**, 375102.

8 I. Sur, D. Cam, M. Kahraman, A. Baysal and M. Culha, *Nanotechnology*, 2010, **21**, 175104.
9 U. Chatterjee, S. Jewrajka and S. Guha, *Polym. Compos.*, 2009, **30**, 827.
10 M. Carbone, D. Donia, G. Sabbatella and R. Antiochia, *J. King Saud Univ., Sci.*, 2016, **28**, 273.
11 S. Lee, H. Kim, R. Patel, S. Im, J. Kim and B. Min, *Polym. Adv. Technol.*, 2007, **18**, 562.
12 A. Pich, A. Karak, Y. Lu, A. Ghosh and H. Adler, *Macromol. Rapid Commun.*, 2006, **27**, 344.
13 Y. Dong, Y. Ma, T. Zhai, F. Shen, Y. Zeng, H. Fu and J. Yao, *Macromol. Rapid Commun.*, 2007, **28**, 2339.
14 G. V. Ramesh, B. Sreedhar and T. P. Radhakrishnan, *Phys. Chem. Chem. Phys.*, 2009, **11**, 10059.
15 T. Wu, Z. Ge and S. Liu, *Chem. Mater.*, 2011, **23**, 2370.
16 V. Skorokhoda, Y. Melnyk, N. Semenyuk, N. Ortynska and O. Suberlyak, *Chem. Chem. Technol.*, 2017, **11**, 171.
17 V. Skorokhoda, Y. Melnyk, V. Shalata, T. Skorokhoda and S. Suberliak, *East.-Eur. J. Enterp. Technol.*, 2017, **1**, 50.
18 V. Skorokhoda, N. Semenyuk, I. Dziaman and O. Suberlyak, *Chem. Chem. Technol.*, 2016, **10**, 187.
19 E. Benetti, X. Sui, S. Zapotoczny and G. Vancso, *Adv. Funct. Mater.*, 2010, **20**, 939.
20 S. Gupta, P. Uhlmann, M. Agrawal, S. Chapuis, U. Oertel and M. Stamm, *Macromolecules*, 2008, **41**, 2874.
21 S. Gupta, M. Agrawal, M. Conrad, N. Hutter, P. Olk, F. Simon, L. Eng, M. Stamm and R. Jordan, *Adv. Funct. Mater.*, 2010, **20**, 1756.
22 S. Konnova, A. Danilushkina, G. Fakhrullina, F. Akhatova, A. Badrutdinov and R. Fakhrullin, *RSC Adv.*, 2015, **5**, 13530.
23 A. Skirtach, A. Antipov, D. Shchukin and G. Sukhorukov, *Langmuir*, 2004, **20**, 6988.
24 M. He, Q. Wang, J. Zhang, W. Zhao and C. Zhao, *ACS Appl. Mater. Interfaces*, 2017, **9**, 44782.
25 T. Wei, Z. Tang, Q. Yu and H. Chen, *ACS Appl. Mater. Interfaces*, 2017, **9**, 37511.
26 X. Wang, S. Yan, L. Song, H. Shi, H. Yang, S. Luan, Y. Huang, J. Yin, A. Khan and J. Zhao, *ACS Appl. Mater. Interfaces*, 2017, **9**, 40930.
27 R. Hu, G. Li, Y. Jiang, Y. Zhang, J. Zou, L. Wang and X. Zhang, *Langmuir*, 2013, **29**, 3773.
28 H. Yang, G. Li, J. Stansbury, X. Zhu, X. Wang and J. Nie, *ACS Appl. Mater. Interfaces*, 2016, **8**, 28047.
29 Y. Stetsyshyn, K. Awsiuk, V. Kusnezh, J. Raczkowska, B. R. Jany, A. Kostruba, K. Harhay, H. Ohar, O. Lishchynskyi, Y. Shymborska, Y. Kryvenchuk, F. Krok and A. Budkowski, *Appl. Surf. Sci.*, 2019, **463**, 1124.
30 J. Raczkowska, Y. Stetsyshyn, K. Awsiuk, M. Brzychczy-Włoch, T. Gosiewski, B. Jany, O. Lishchynskyi, Y. Shymborska, S. Nastyshyn, A. Bernasik, H. Ohar, F. Krok, D. Ochońska, A. Kostruba and A. Budkowski, *Mater. Sci. Eng., C*, 2019, **103**, 109806.
31 K. McNamara and S. Tofail, *Adv. Phys.: X*, 2017, **2**, 54.
32 M. Azizi, H. Ghourchian, F. Yazdian, S. Bagherifam, S. Bekhradnia and B. Nyström, *Sci. Rep.*, 2017, **7**, 5178.
33 T. Zhang, L. Wang, Q. Chen and C. Chen, *Yonsei Med. J.*, 2014, **55**, 283.
34 F. Liu, M. Mahmood, Y. Xu, F. Watanabe, A. Biris, D. Hansen, A. Inselman, D. Casciano, T. Patterson, M. Paule, W. Slikker and C. Wang, *Front. Neurosci.*, 2015, **9**, 115.
35 S. Edmondson and B. Zhu, *Mater. Sci.*, 2012, 12–14.
36 A. Kostruba, M. Ohar, B. Kulyk, O. Zolobko and Y. Stetsyshyn, *Appl. Surf. Sci.*, 2013, **276**, 340.
37 A. Kostruba, Y. Stetsyshyn and R. Vlokh, *Appl. Opt.*, 2015, **54**, 6208.
38 S. Kasraei and M. Azarsina, *Braz. Oral Res.*, 2012, **26**, 505.
39 R. Jagtap and A. Ambre, *Indian Journal of Materials Science*, 2013, **13**, 368.
40 K. Awsiuk, A. Bernasik, M. Kitsara, A. Budkowski, J. Rysz, J. Haberko, P. Petrou, K. Beltsios and J. Raczkowska, *Colloids Surf., B*, 2010, **80**, 63.
41 M. Marrese, V. Guarino and L. Ambrosio, *J. Funct. Biomater.*, 2017, **8**, 7.
42 S. Malynych, A. Luzinov and G. Chumanov, *J. Phys. Chem.*, 2002, **106**, 1280.
43 S. Nam, D. V. Parikh, B. D. Condon, Q. Zhao and M. Yoshioka-Tarver, *J. Nanopart. Res.*, 2011, **13**, 3755.
44 S. Gurunathan, M. Qasim, C. Park, H. Yoo, D. Choi, H. Song, C. Park, J.-H. Kim and K. Hong, *Int. J. Mol. Sci.*, 2018, **19**, 3618.
45 M. Akter, M. T. Sikder, M. M. Rahman, A. K. M. A. Ullah, K. F. B. Hossain, S. Banik, T. Hosokawa, T. Saito and M. Kurasaki, *J. Adv. Res.*, 2018, **9**, 1.
46 W. Liu, Y. Wu, C. Wang, H. C. Li, T. Wang, C. Y. Liao, L. Cui, Q. F. Zhou, B. Yan and G. B. Jiang, *Nanotoxicology*, 2010, **4**, 319.
47 P. Rajanahalli, C. J. Stucke and Y. Hong, *Toxicol. Rep.*, 2015, **2**, 758.
48 M. Milić, G. Leitinger, I. Pavičić, M. Zebić Avdičević, S. Dobrović, W. Goessler and I. Vinković Vrček, *J. Appl. Toxicol.*, 2015, **35**, 581–592.
49 J. Han, S. Gurunathan, Y. Choi and J. Kim, *Int. J. Nanomed.*, 2017, **12**, 7529.
50 S. Gurunathan, J. W. Han, V. Eppakayala, M. Jeyaraj and J.-H. Kim, *BioMed Res. Int.*, 2013, **2013**, 535796.
51 S. F. Hansen, B. H. Larsen, S. I. Olsen and A. Baun, *Nanotoxicology*, 2007, **1**(3), 243.
52 SCENIHR, Scientific Committee on Emerging and Newly Identified Health Risks, *SCENIHR Opinion on Nanosilver: safety, health and environmental effects and role in antimicrobial resistance*, 1. 06. 2014, ISSN: 831-4783.
53 S. F. Hansen, E. S. Michelson, A. Kamper, P. Borling, F. Stuer-Lauridsen and A. Baun, *Ecotoxicology*, 2008, **17**, 438.

